ANALYSIS OF SIMULATED TEMPORAL ILLUMINATION AT THE LUNAR PSRS T. J. Thompson[1], P. Mahanti[1], The LROC Team [1]Lunar Reconnaissance Orbiter Camera, School of Earth and Space Exploration, Arizona State University, Tempe, AZ, USA (tthompson@ser.asu.edu);

Introduction: The Moon's lower range of sub-solar latitudes (-1.5° to 1.5°) through the seasons and longer days distinguish lunar lighting conditions from those of Earth. The absence of atmosphere means most of the incident photon flux impinging upon the Moon reaches the surface.

Some areas of the lunar surface never receive direct illumination (permanently shadowed regions, PSRs) [1] and have drawn illumination modeling interest [2], with emphasis on conditions for ice stability [3]. Furthermore, the absence of atmosphere also means the absence of light getting scattered by air, thus the common secondary illumination is from ground scattered light.

How bright are areas such as crater walls that can be seen from an arbitrary observer location, such as the bottom of a PSR? To answer this, we simulate lighting and only select areas visible to the observer. To further understanding of the topographic influence on the secondary illumination we calculate viewfactors [4] for all surfaces in the map. For our viewfactor maps, each cell value is the fraction of incident light at that cell which will go on to intersect another cell. This method requires DTMs, sub-solar points, and points of interest (receiver locations). So while this approach was designed with PSRs in mind, it may be used in other contexts.

Temporal Trends in Primary Illumination Within Line of Sight: We employ existing methods [5] to simulate surface lighting (cosine of incidence angle) and collect statistics for the set of pixels within the viewshed of an observer. First, sub-solar points are calculated using SPICE [6] through WebGeocalc (https://naif.jpl.nasa.gov/naif/webgeocalc.html) over a time period of interest. The illumination simulation program map_illum_layer [5] requires the sub-solar point to compute a solar vector. The angle between this vector and the surface normal is the incidence, i. The surface is modeled as brighter at smaller incidence angles, where the cell value, v is determined by $v = cos(i) \times 255$. Lunar Orbiter Laser Altimeter (LOLA) data [7] is used poleward of 79°latitude as the elevation basemap necessary for calculating shading. One map is created for each of the sub-solar points since the sun position changes with time. A viewshed map is generated for the chosen observer position and multiplied by the illumination map. Unlit pixels and those outside of line of sight are turned null. Summary statistics are calculated for the result of this multiplication. The data for all the output maps is stored as a table so these summary values may be compared across the time range (Figure 1).

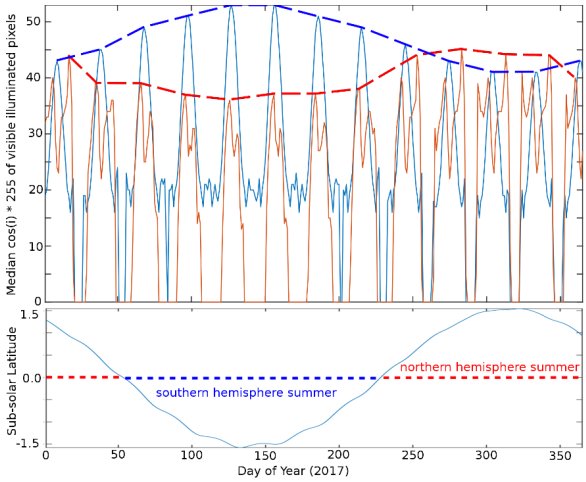

Figure 1: Seasonal relationship between visible, illuminated pixels from the perspective of a location on the floor of a north pole (red, Fibiger) and south pole (blue, Scott) PSR crater simulated for 2017

An example of summary output plots is found in Figure 1. The longest wavelength signal indicated by the dotted lines over the peaks (blue for Scott, red for Fibiger) shows the median value for the set of illuminated pixels within the line of sight of an observer on the floor. The largest median occurs during each pole's respective summer. The individual peaks and valleys trace the lunar day and night. Other peculiarities may be attributed to local topography. Figure 2 illustrates the illumination maps at different times in the lunar day for Fibiger crater, which hosts a north pole PSR.

Topographic Effects on Secondary Illumination: The orientation and position of a light emitter and receiver is key in the secondary flux at the receiver. A viewfactor is the fraction of the incident light on one object output towards another object. This method has been applied in a planetary context by Vasavada et al. [3] for lunar and mercurian craters for computation of thermal balance, but we are using the same principle in the context of secondary illumination in primary shadows. To calculate this coefficient (Eq.1, after [3]) we use the DTM to derive the positions and orientation of all potential emitters compared to the receiver. The DTM is first convolved with 3x3 filters to calculate x and y directional slopes for each pixel. The pixel scale and elevation is used to generate the x direction and y direction vectors which describe an oriented plane. Each

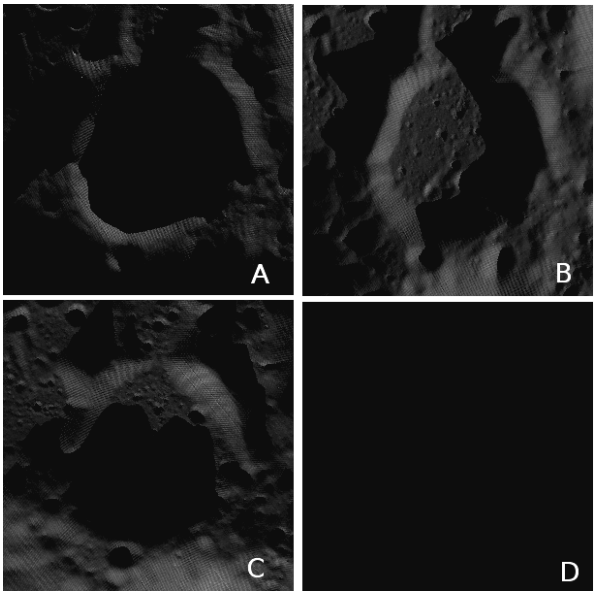

Figure 2: Illumination conditions at the northerly Fibiger crater at 7 day intervals in January 2017. A.) January 1st. B.) January 7th. C.) January 14th. D.) January 21st.

cell or plane in the raster is treated as an emitter. The geometry between the emitter and receiver surface normals and the line of sight between the two are calculated according to Eq 1. Planes that face each other and are close together have larger viewfactor coefficients.

$$a_{ij} = \frac{1}{\pi} \frac{(\cos(\theta_1)\cos(\theta_2)A_2)}{R_{ij}^2} \tag{1}$$

As the whole map contains a_{ij} values, it is then possible to multiply a map containing primary illumination values, I_{ij}, for each cell in the raster, and also an albedo map, q_{ij}, to account for reflectivity. After this element by element multiplication, summing all elements of the matrix gives the total flux at the specified receiver plate. This function calculated for all cells is outlined with equation 2.

$$I_{i_r j_r} = \sum_{i=0}^{n_r-1} \sum_{j=0}^{n_c-1} a_{ij} \times I_{ij} \times q_{ij} \tag{2}$$

The output a_{ij} map is stored as a 32 bit geotiff with the same offsets and pixel scales as the DTM. The a_{ij} values decrease with the square of distance from the receiver. Also, nearby terrain tends to have similar orientations inhibiting received scattered light, as surface normals need to be colinear and opposite for greatest light reception. The expected patterns for lunar craters are low amounts of incident scattered light in the flats due to near-parallel plate orientations and increased incident scattered light where the slopes of the inner wall of the crater are steep, then a fading with distance. Observing Figure 4, receiver 1 tilts towards the top of the

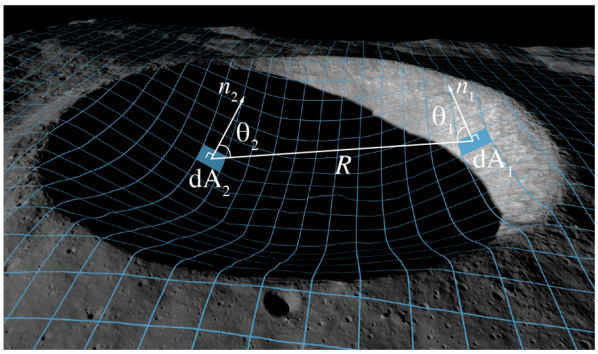

Figure 3: Angular relationship between emitting and receiving planes in a crater demonstrated with a digital model of Sylvester N crater

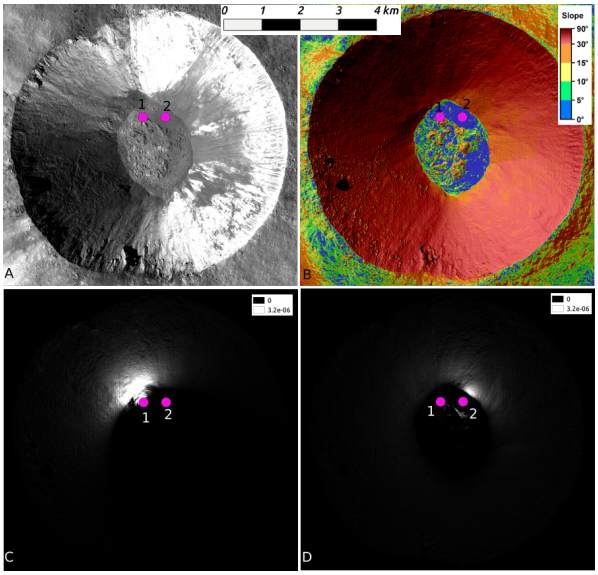

Figure 4: A. 90cm/px Eimmart A narrow angle camera (NAC) image, up is north. The pink dots are receiver 1 and receiver two. B. slope map. C. viewfactor map for receiver 1. D. viewfactor map for receiver 2. Source of imagery, topography, and slopemap from http://wms.lroc.asu.edu/lroc/view_rdr/NAC_DTM_EIMMARTA

image, so it is able to receive light from the floor in front of it, but since the receiver plate is tilted forwards, very little light reaches the receiver from the south. Receiver 2 is on flat ground, thus other flat areas contribute little light, it is the steepness of the nearby wall that contributes most scattered light according to the model.

References: [1] K. Watson, et al. (1961) *JGR* 66(9):3033. [2] E. Mazarico, et al. (2011) *Icarus* 211(2):1066. [3] A. R. Vasavada, et al. (1999) *Icarus* 141(2):179. [4] D. C. Hamilton, et al. (1952) . [5] C. Hanger, et al. (2013) in *Lunar Science Forum*. [6] C. Acton, et al. (2016) *ISPRS* 357–359. [7] D. E. Smith, et al. (2010) *Geophysical Research Letters* 37(18).